Significant impact of lithogenic dissolution from subantarctic volcanic islands on the regional marine silicon cycle

Edwin Cotard, Valentin Deteix, Frédéric Vivier, Arnaud Dapoigny, Sandrine Caquineau, Damien Cardinal

LIMNOLOGY and OCEANOGRAPHY

ASLO

Limnol. Oceanogr. 9999, 2025, 1–14

doi: 10.1002/lno.70243

RESEARCH ARTICLE

Significant impact of lithogenic dissolution from subantarctic volcanic islands on the regional marine silicon cycle

Edwin Cotard,[1*] **Valentin Deteix**,[1] **Frédéric Vivier**,[1] **Arnaud Dapoigny**,[2] **Sandrine Caquineau**,[1] **Damien Cardinal**[1*]

[1]LOCEAN-IPSL (Sorbonne Université, IRD, CNRS, MNHN), Paris, France; [2]LSCE-IPSL (Paris Saclay, CEA, CNRS, UVSQ), Saint-Aubin, France

Abstract

Silicic acid controls the production of diatoms, a predominant phytoplankton in the Southern Ocean. Diatoms are major contributors to the biological carbon pump, which is particularly active in the Southern Ocean as well as in areas naturally enriched in iron, such as around the Kerguelen Plateau. This study evaluates the factors controlling the biogeochemical cycle of Si and its dynamics in this area and how it is impacted by the island mass effect using the Si isotopic signatures of both dissolved and biogenic Si. While subsurface winter waters have similar δ^{30}Si signatures and dissolved Si concentrations, surface δ^{30}Si and dissolved Si values are different between stations. We show that this results from both (i) a different degree of dissolved Si utilization by silicifiers from winter water as the main Si source and (ii) an additional significant Si source to dissolved Si in the mixed layer from lithogenic Si dissolution for areas under the influence of the shelf. Indeed, the $\delta^{30}Si_{DSi}$ signatures near the islands are homogeneous and lighter by $-0.33‰ \pm 0.07‰$ in the mixed layer compared to the outside plateau station. We estimate such lithogenic Si contribution to dissolved Si at 2.9 ± 1.8 μmol L^{-1} for a corresponding specific flux of $3.7 \pm 2.3 \times 10^6$ mol km^{-2} yr^{-1} in shallow areas around Heard and McDonald Islands (< 100 m). This Si dissolution flux per surface area is among the highest in the ocean and has a traceable biogeochemical impact over the Northern Kerguelen Plateau. It is likely due to the active volcanic nature of these islands combined with subglacial erosion on Heard.

Silicon (Si) is a key element for silicifying marine organisms. In the form of silicic acid (dissolved Si, DSi), Si controls the production of diatoms, which are the predominant phytoplankton in the Southern Ocean (e.g., Brzezinski et al. 2001; Tréguer and De La Rocha 2013). Diatoms are key players in the biological carbon and silicon pumps (Tréguer et al. 2018), which are particularly active in the Southern Ocean, including in the naturally iron-rich zones around the sub-Antarctic and Antarctic islands (Blain et al. 2007; Closset et al. 2014). The biological carbon pump is a crucial process in the oceanic carbon cycle, contributing to the sequestration of ca. 13 PgC yr^{-1} (Khatiwala et al. 2009; Bouttes et al. 2012), although it remains poorly quantified, with a large spread of estimates (Wang et al. 2023). The biological carbon pump is often associated with biogenic silica (BSi) export to deep waters via diatom frustules (Dugdale et al. 1995), making the Southern Ocean a significant contributor to the global carbon and silicon cycles and thus to climate (Tréguer et al. 2021).

The Southern Ocean, covering 20% of the World Ocean, is predominantly a HNLC region (High Nutrient Low Chlorophyll), with primary production co-limited by the availability of light and micronutrients such as iron (Dugdale et al. 1995; Quéguiner and Brzezinski 2002). South of the Polar Front in the Antarctic Zone, iron concentrations are very low (< 1 nmol L^{-1}, Tagliabue et al. 2012), and diatoms are very abundant (e.g., Armand et al. 2005; Kopczyńska et al. 2007; Closset et al. 2015). In fact, their productivity in this zone represents one third of the silica production in the World Ocean (Buesseler et al. 2001; Quéguiner and Brzezinski 2002; Tréguer and De La Rocha 2013). The distribution of silicon at the

*Correspondence: cotard.edwin@gmail.com; damien.cardinal@sorbonne-universite.fr

Associate editor: Robinson Fulweiler

surface is constrained by the upwelling of nutrients at the Antarctic divergence, then transported northward by Ekman transport and consumed by diatoms (Brzezinski et al. 2001; Quéguiner and Brzezinski 2002). Indeed, this upper limb of the meridional overturning circulation redistributes nutrients toward low latitudes where the biological carbon pump is therefore Si limited relative to nitrogen (Moore et al. 2001, 2004; Sarmiento et al. 2004, 2007).

In the Antarctic Zone of the Southern Ocean (south to the Polar Front), the surface dissolved Si availability is also controlled by the formation of winter water (WW). Winter water corresponds to a subsurface temperature minimum visible during the austral summer as a remanence of the deep winter mixed layer (Park et al. 1998). As such, dissolved Si concentration in WW can be considered representative of winter surface Si stocks and as the source of Si for the surface waters, prior to the summer restratification (e.g., Trull et al. 2001; Cardinal et al. 2005; Fripiat et al. 2011b, 2011a). The dissolved Si concentrations in the mixed layer (ML) of the Antarctic Zone are generally non-limiting for diatoms. However, in specific environments, such as areas naturally fertilized with micronutrients like iron, the dissolved Si may limit or co-limit the development of silicifying phytoplankton at specific periods such as the end of summer (Mosseri et al. 2008; Closset et al. 2014; Geisen et al. 2022). In this study, we focus on the Kerguelen Plateau, including the coastal areas of Heard and McDonald Islands (HMI), which are particularly dynamic environments (e.g., Park et al. 2008) and naturally Fe fertilized (e.g., Blain et al. 2007). Consequently, a large seasonal phytoplankton bloom dominated by diatoms takes place in the region (Armand et al. 2008; Mosseri et al. 2008). The main source of dissolved Si there is attributed to the mixing of the silicon-rich WW (Fripiat et al. 2011a, 2011b). However, other sources have been suggested as potentially significant, particularly in late summer when dissolved Si becomes limiting: aerosols (Heimburger et al. 2013), basaltic weathering (Fripiat et al. 2011b), volcanic ashes (Geisen et al. 2022; Deteix et al. 2024). These different silicon inputs and the efficiency of the use of the dissolved Si reservoir are difficult to discriminate and quantify.

The measurement of stable silicon isotopes (^{28}Si, ^{29}Si, ^{30}Si) signatures, referred to as $\delta^{30}Si$ provides essential information for a better understanding of these key environments. Indeed, diatoms preferentially assimilate light silicon isotopes, thus enriching the dissolved Si stock in surrounding waters with the heavy isotopes while biogenic Si resulting from opal formation by diatoms has a marked isotopic fingerprint (e.g., Varela et al. 2004; Cardinal et al. 2007). The Si isotopic enrichment factor of diatoms' uptake, $^{30}\varepsilon$, was first established at a mean value of $-1.1‰ \pm 0.2‰$ for diatoms (de la Rocha et al. 1997). Compiling data from the ACC, the mean $^{30}\varepsilon$ value was estimated at $-1.2‰ \pm 0.2‰$ (De La Rocha et al. 2011; Fripiat et al. 2011b). Most results from different ACC samples confirmed this mean in situ fractionation factor estimate (e.g., Closset et al. 2016).

In this study, we focus on the biogeochemical province south of the Polar Front and around the Kerguelen Plateau with an unprecedented spatial resolution, including around HMI that both have active volcanoes. Our goals are to better characterize the island mass effects on the plateau and its impact on the distribution of Si and include (i) the identification of dissolved Si sources and sinks and (ii) the quantification of the dissolution fluxes of lithogenic Si (LSi) on the Kerguelen Plateau from Heard and McDonald shoal.

Materials and methods

Study site: Antarctic zone of the south-west Indian Ocean GEOTRACES section GS02 (SWINGS)

The SWINGS cruise took place during the austral summer onboard R/V *Marion Dufresne* along a transect in the south-west Indian Ocean. On this transect, 11 stations were sampled for dissolved Si and biogenic Si in the Antarctic zone from 15 February to 27 February 2021 (Table 1; Fig. 1). Seven shelf stations (44, 45, 46, 65, 66, 67, and 68) were identified as being above the geomorphologically unique Northern Kerguelen Plateau (bottom depth < 500 m) and potentially naturally fertilized with micronutrients.

The shelf stations are distributed along an arc following the geostrophic circulation over the plateau from Heard to Kerguelen Islands (Park et al. 2008) and were sampled within the bloom (Fig. 1). Note that Station 68 in our study is at the same location as the A3 station of the KEOPS and KEOPS-2 cruises (Blain et al. 2007; Closset et al. 2016). In addition, some stations were chosen to be as close as possible to the islands in their coastal zone: Stations 45 and 46 for Heard Island and 65 for McDonald (Table 1). These two islands are volcanically active, in contrast to Kerguelen. Glaciers are present on the Kerguelen and Heard islands but not on McDonald. Four stations (42, 47, 58, 63) are located outside the Kerguelen Plateau (Table 1). Note that Station 42 was also sampled during the KEOPS-2 campaign (labeled Kerfix). Station 47 is located in the Southern Enderby Basin, at the southeastern edge of the Kerguelen Plateau. Station 58, located in the Australian Antarctic Basin, is the southernmost station on the SWINGS transect. Finally, Station 63 is located in the core of the Fawn Trough Current (FTC), where one third of the ACC flows and divides the Kerguelen Plateau into two zones (Park et al. 2009).

Isotopic measurements

Sample collection, methodology for biogenic Si and lithogenic Si concentrations are from Deteix et al. (2024) and are briefly described in Supporting Information Text S1 as well as the sample preparation for Si isotopes which is based on well-established methods (MAGIC protocol, Karl and Tien 1992; Reynolds et al. 2006). Parameters for analytical measurements of Si isotopic compositions ($\delta^{30}Si$) are detailed in Supporting Information Text S2. The mass dependence of the fractionation is checked by ensuring that $\delta^{30}Si$ vs. $\delta^{29}Si$ ratios

Table 1. Stations are classified into different categories: Northern Enderby Basin, Southern Enderby Basin, Australian Antarctic Basin, Fawn Trough for stations deeper than 1000 m and HMI (Heard–McDonald Islands) Trough, HMI Shoal and KI (Kerguelen Island) Trough for stations shallower than 500 m. The mixed layer depth (MLD), determined from visual inspection of temperature, salinity, and density anomaly profiles, with the density criteria of 0.03 kg m^{-3} (De Boyer Montégut et al. 2004), and the winter water (WW) depth determined from visual inspection of the subsurface temperature minimum. For a detailed map of the different sub-areas, the reader is referred to Supporting Information Fig. S1.

Station	Sub-area	Over/outside Northern Kerguelen Plateau	Sampling date	Bottom depth (m)	MLD (m)	WW (m)
42	Northern Enderby Basin (Kerfix, KEOPS-2)	Outside	15/02/21	1690	107	201
44	HMI Trough	Over	17/02/21	289	80	na
45	HMI Shoal	Over	18/02/21	82	82	na
46	HMI Shoal	Over	18/02/21	116	66	na
47	Southern Enderby Basin	Outside	18/02/21	2139	126	198
58	Australian Antarctic Basin	Outside	22/02/21	2087	53	80
63	Fawn Trough	Outside	24/02/21	2399	97	130
65	HMI Shoal	Over	26/02/21	138	22	na
66	HMI Trough	Over	26/02/21	409	108	180
67	HMI Trough	Over	26/02/21	420	116	150
68	KI Trough (A3, KEOPS and KEOPS-2)	Over	27/02/21	479	100	180

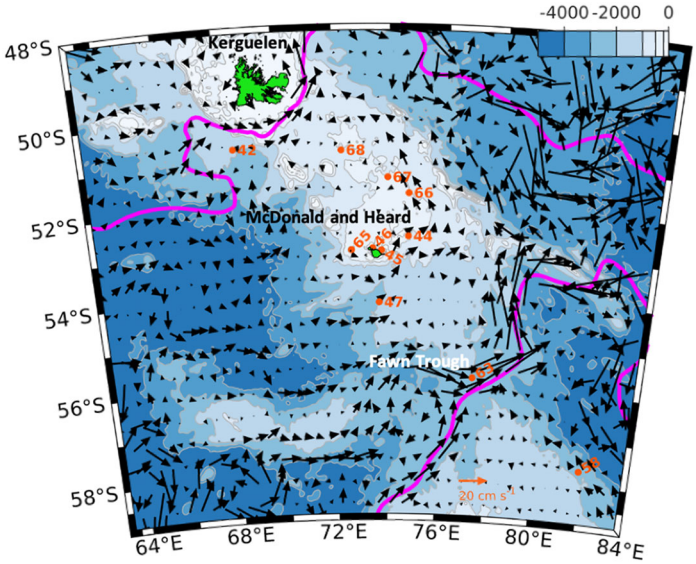

Fig. 1. Selected hydrographic stations with Si sampling during the SWINGS cruise between 15 and 27 February 2021. Bathymetry, represented by a blue color scale, is from the ETOPO1 global relief model. The Polar Front and the Southern ACC Front, as determined by Park et al. (2019), are indicated by magenta lines. Arrows denote the average satellite-derived surface geostrophic velocity field between 16 and 27 February 2021. Green areas represent Kerguelen, Heard, and McDonald Islands.

plot on a mass fractionation line (Supporting Information Fig. S2), precluding significant isobaric interferences.

Before each session and regularly during the analysis sessions, Diatomite, a secondary reference material, was measured: $\delta^{30}Si_{diat} = 1.26‰ \pm 0.10‰$ (Reynolds et al. 2007). Over the 2 yr of analysis of this dataset, the Diatomite values are 1.22‰ ± 0.05‰ (1sd, $n = 50$). In addition, another secondary reference material (seawater GEOTRACES Aloha, 1000 m) was also measured, $\delta^{30}Si_{Aloha1000} = 1.24‰ \pm 0.10‰$ (Grasse et al. 2017). Over the 2 yr of analysis of this dataset, the $Aloha_{1000}$ values are 1.20‰ ± 0.05‰ (1sd, $n = 15$). Chemical and analytical replicates were also measured over separate sessions for most samples (89% of $\delta^{30}Si_{DSi}$ and 71% of $\delta^{30}Si_{BSi}$ samples replicated). The average measured reproducibility for $\delta^{30}Si_{DSi}$ is 0.07‰ (1sd, $n = 80$) and 0.05‰ for $\delta^{30}Si_{BSi}$ (1sd, $n = 30$). Note that there was no difference between analytical reproducibility (single chemical processing of one sample with several analyses of the same solution) and full replicates (several chemical purifications), suggesting that most of the uncertainty comes from the isotopic measurement itself.

Complementary data sets and isotopic models used (open steady state and Rayleigh models) as well as the calculation for isotopic mass balance are explained in the Supporting Information, respectively Supporting Information Text S3 and S4.

Results

We observed a typical depletion of dissolved Si concentrations toward the surface and a shallower silicicline toward the south of the transect while the dissolved Si (DSi) isotopic signature becomes heavier as its concentration decreases because of the isotopic fractionation at the surface due to the preferential uptake of light isotopes by diatoms (Fig. 2).

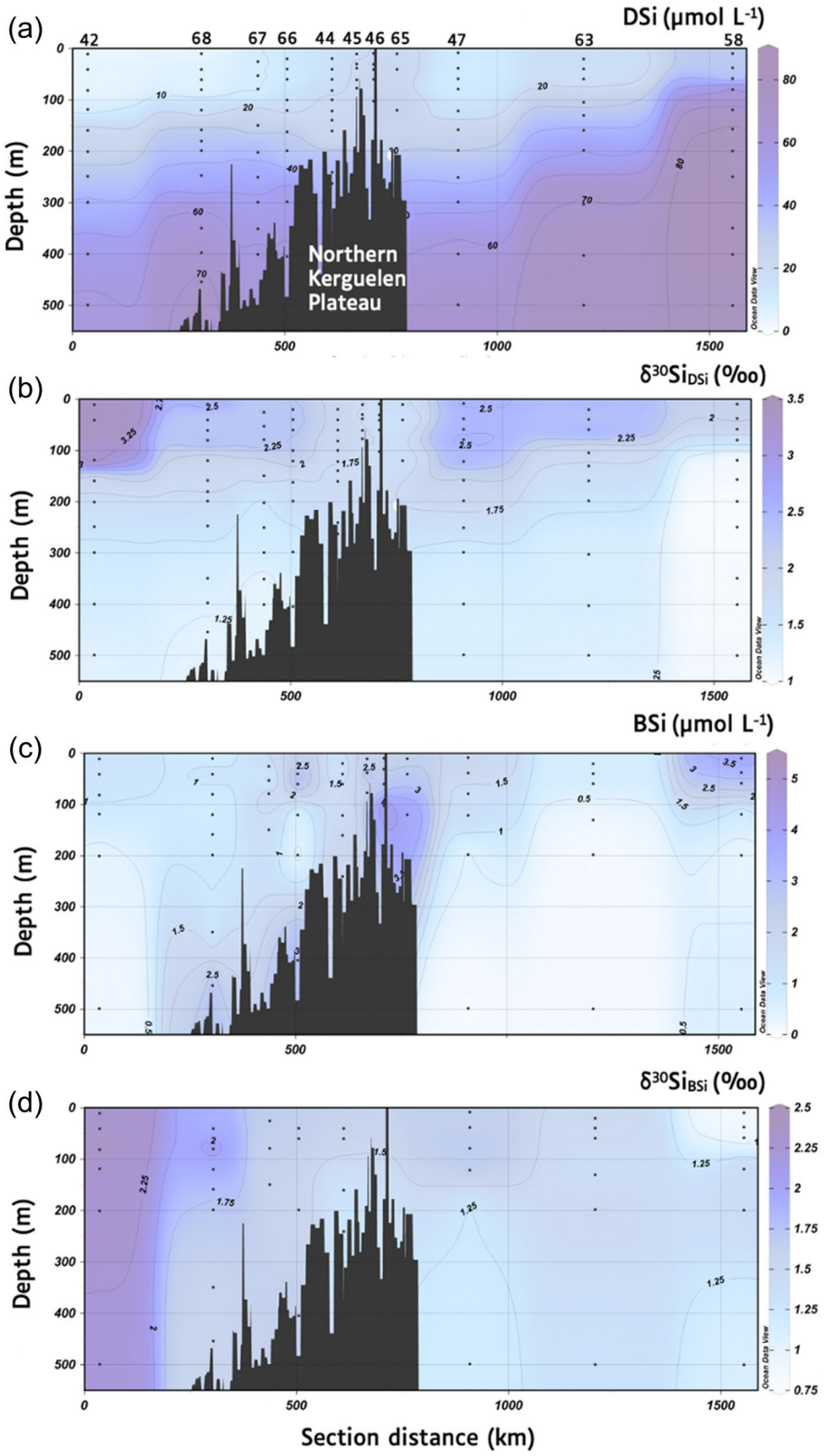

Fig. 2. Sections of (**a**) dissolved Si concentrations, (**b**) $\delta^{30}Si_{DSi}$, (**c**) biogenic Si (BSi) concentrations from Deteix et al. (2024) and (**d**) $\delta^{30}Si_{BSi}$, of the SWINGS stations south of the Polar Front, around the Kerguelen Plateau. Graphics from Ocean Data View (Schlitzer 2024).

Outside plateau stations (42, 47, 58, and 63)

The surface-bottom gradient is particularly marked between Stations 42 and 58 (Fig. 2; Supporting Information Fig. S3). Outside Plateau stations are compared with three stations from the KEOPS, KEOPS-2, and ANTXXIII/9 cruises, respectively (Supporting Information Fig. S3). Surface dissolved Si concentrations are higher toward the south, ranging from less than 5 μmol L^{-1} to more than 25 μmol L^{-1} (Fig. 2a; Supporting Information Fig. S3a). Surface $\delta^{30}Si_{DSi}$ values range between 3.38‰ and 2.07‰ for Stations 42 and 58, respectively. The values then homogenize around 1.28‰ ± 0.03‰ at 500 m, except for Station 58 with light signatures around 1.0‰ down to 100 m (Fig. 2b; Supporting Information Fig. S3b). These results are consistent with the concentration and isotopic ranges found during the cruises over a similar study area, except for the signatures from Station 42, which are significantly heavier by 1‰ at the surface (Fig. 2; Supporting Information Fig. S3; Supporting Information Table S1).

As discussed in Deteix et al. (2024), biogenic Si (BSi) concentrations generally decrease with depth over the first 500 m, with a marked gradient at Station 58 where we observe a high biogenic Si patch exceeding 3 μmol L^{-1} in the first 60 m (Fig. 2c; Supporting Information Fig. S3c). The isotopic signatures of biogenic Si at the surface are contrasted, with differences of more than 1.5‰ between Stations 58 and 42 (Fig. 2d; Supporting Information Fig. S3d). This distribution is inversely proportional to biogenic Si concentrations. Isotopic signatures at Station 58 are particularly light (< 0.9‰), while they are heavier for Station 42 (> 2.3‰) (Fig. 2d; Supporting Information Fig. S3d). For Stations 47 and 63 (FTC), the biogenic Si signatures are around 1.6‰ and remain homogeneous over the first 500 m (Fig. 2d). The data measured during the KEOPS cruises are similar in concentration and isotopic signatures, except for one point at 150 m at Station A11 (KEOPS), where the concentration is higher and the isotopic signature is lighter, as well as R2 (KEOPS-2), $\delta^{30}Si_{BSi}$ < 0.8‰ (Supporting Information Fig. S3c,d).

Over plateau stations (44, 45, 46, 65, 66, 67, and 68)

Compared with the non-plateau stations, dissolved Si concentrations in the ML of the plateau stations are more homogeneous, with a variability of ± 7 μmol L^{-1} (1sd) compared with ± 12 μmol L^{-1} (1sd) for the so-called outside plateau stations (Fig. 2; Supporting Information Table S1). Surface concentrations range from 23 to 5 μmol L^{-1} at Stations 65 (McDonald) and 68 (A3, Kerguelen), respectively (Supporting Information Fig. S4a). Around Heard Island, dissolved Si concentrations are particularly homogeneous and relatively high (> 20 μmol L^{-1}), and are associated with a light isotopic anomaly in the ML, compared to outside plateau stations (Fig. 2a,b; Supporting Information Fig. S4a). This anomaly extends over all stations with a bottom depth shallower than 150 m (stations 45, 46, and 65) which have a dissolved Si isotopic signature of 1.70‰ ± 0.14‰ (Fig. 2b; Supporting Information Fig. S4b).

For stations with bottom depth between 150 and 500 m, dissolved Si surface concentrations range from 6 μmol L^{-1} (Station 68) to 15 μmol L^{-1} (Station 44). As for the outside plateau stations, the values homogenize with depth, with values exceeding 60 μmol L^{-1} below 400 m (Fig. 2a; Supporting Information Fig. S4a). The resulting isotopic signatures in the ML are 2.23‰ ± 0.17‰ and tend toward a value lighter than 1.5‰ with depth. The SWINGS values on the Kerguelen Plateau are homogeneous and consistent with those from KEOPS Station A3 (Supporting Information Fig. S4a,b).

Biogenic Si concentrations are described in Deteix et al. (2024). Their Si isotopic compositions are more variable than $\delta^{30}Si_{DSi}$. Stations 44, 66, and 67 have very homogeneous $\delta^{30}Si_{BSi}$ values at 1.62‰ ± 0.03‰ in the ML (Supporting Information Fig. S4d) and are homogeneous throughout the water column for Stations 66 and 67. The biogenic Si isotopic signatures for Station 68 are heavier: 2.00‰ (Fig. 2b; Supporting Information Fig. S4d). For Stations 44 and 68, the biogenic Si isotopic data are close to the dissolved Si isotopic data and lighten with depth (Fig. 2b,d; Supporting Information Fig. S4b,d). The biogenic Si SWINGS isotopic values are similar to those from Station A3 KEOPS (also corresponding to a summer sampling) and are more than 1‰ heavier than the spring data from KEOPS-2 at A3 (Supporting Information Fig. S4d).

Winter water

Winter waters are often used as the sole source of Si in steady state and Rayleigh models in the Southern Ocean (e.g., Cardinal et al. 2005; Fripiat et al. 2011b; Closset et al. 2016), since they are representative of the initial conditions before summer stratification (Park et al. 2014; Blain et al. 2015). We compile in Table 2 $\delta^{30}Si_{DSi}$ signatures of WWs with their associated dissolved Si concentrations from different campaigns in the Antarctic Zone.

While most of the values converge toward isotopic signatures around 1.5‰ to 1.7‰ and dissolved Si concentrations between 30 and 40 μmol L^{-1}, we note a greater variability in certain dissolved Si and $\delta^{30}Si_{DSi}$ values in the WW. This is particularly noticeable for the southernmost cruises, as expected since they are closer to the Antarctic divergence upwelling; therefore, with higher concentrations and isotopically lighter dissolved Si.

Nevertheless, the data for the Kerguelen Plateau are similar between the KEOPS and SWINGS surveys, with no significant difference between the on-plateau and outside-plateau stations for SWINGS (excluding Station 58). The variation in dissolved Si in WW is significant due to the relatively large area covered; however, the isotopic variations remain remarkably small. Therefore, in the following, we test a single WW source (Fig. 3a).

Table 2. Dissolved Si concentrations and $\delta^{30}Si_{DSi}$ in WW for SWINGS stations (42, 47, 58, 63, 66, 67, and 68) and average on plateau and out plateau compared with various oceanographic campaigns.

WW	On plateau, average	Out plateau, average, without 58	42 Out plateau	47 Out plateau	58 Out plateau	63 Out plateau	66 On plateau	67 On plateau	68 On plateau
$\delta^{30}Si_{DSi}$ (‰)	1.76 ± 0.06	1.74 ± 0.09	1.68	1.84	1.51	1.70	1.70	1.81	1.78
DSi (μmol L^{-1})	31.6 ± 4.3	29.1 ± 4.8	24.1	29.7	64.2	33.7	32.1	27.0	35.6

	SWINGS, average (this study)		KEOPS-2*		KEOPS†					
WW	58	All data, without 58	On plateau	Out plateau	On plateau	Out plateau	ANTXXIII/9‡	BONUS-GH§	EIFEX‖	CLIVAR-SR3¶
$\delta^{30}Si_{DSi}$ (‰)	1.51	1.75 ± 0.07	1.76 ± 0.03	1.71 ± 0.03	1.9 ± 0.1	1.5 ± 0.0	1.2–1.7	1.57 ± 0.33	1.6 ± 0.2	1.3 ± 0.2
DSi (μmol L^{-1})	64.2	30.3 ± 4.3	31.6 ± 2.2	32.9 ± 2.2	34.2 ± 1.9	52.5 ± 3.3	45–90	59 ± 22	37.3 ± 2.8	60.9 ± 9.3

*Closset et al. (2016): October–November 2011.
†Fripiat et al. (2011b): January–February 2005.
‡Coffineau et al. (2014); De La Rocha et al. (2011): February–April 2007.
§Fripiat et al. (2011a): February–March 2008.
‖(Cavagna et al. 2011): January–March 2004.
¶Cardinal et al. (2005): November 2001.

Dynamics of surface processes

We distinguish two different trends between over and outside plateau stations for ML $\delta^{30}Si_{DSi}$ vs. dissolved Si concentration for the SWINGS, KEOPS, and KEOPS-2 cruises (Fig. 3). This suggests two distinct isotopic systems: outside-plateau stations (42, 47, 58, and 63) and on-plateau stations (44, 45, 46, 65, 66, 67, and 68). *See* the Supplementary Text S3 for a general description of Rayleigh and steady-state isotopic models and their equations. The stations over plateau or coastal influence are, on average, 0.58‰ lighter compared to outside-plateau stations (Fig. 3a; Supporting Information Table S1).

Outside plateau stations (42, 47, 58, and 63)

Using the mean values of the WWs (Table 2), either Rayleigh or steady state cannot explain the use of the dissolved Si reservoir in the mixed layer for all the outside-plateau stations (notably Station 42; Fig. 3a). This is different from the KEOPS HNLC stations that could be systematically explained by a single steady state model (Fripiat et al. 2011b). The mixed-layer isotopic signatures at Station 47, located at the southern end of the Kerguelen Plateau, can be fully described by a steady state model (Fig. 3a), which may be induced by repeated mixing events at depth supplying nutrients to the surrounding surface water (Park et al. 2008). The surface isotopic signatures from Station 63, in the core of the Fawn Trough Current, are more consistent with a Rayleigh model, but if the uncertainty in $^{30}\varepsilon$ is taken into account, the values are also very close to the steady-state model (Fig. 3a). This is due to a small f (low relative use of dissolved Si) making both the Rayleigh and steady-state models indistinguishable. However, two stations (42 and 58) are atypical and are processed separately in Supporting Information Text S5 and Supporting Information Fig. S5.

Over plateau stations (44, 45, 46, 65, 66, 67, and 68)

Compared with the theoretical steady state model, calculated with the mean SWINGS WW as Si-source, the on-plateau surface signatures are 0.33‰ ± 0.07‰ lighter on average (Fig. 3a) and cannot explain the plateau isotopic signatures. During the KEOPS cruise, a similar finding had been reported for the closest station to Heard Island (C1) and was suggested to originate from a basaltic input (Fripiat et al. 2011b). A closer look at Station A3 KEOPS shows that the Si isotopic signature is also lighter than expected (Fig. 3a).

Moreover, the SWINGS plateau ML dissolved Si isotopic signatures display a very good linear correlation with DSi concentration, including data from A3 KEOPS (Fig. 3a), whereas no light isotopic anomalies were observed during KEOPS-2 (Closset et al. 2016). The KEOPS-2 cruise did not extend to the south-east of the plateau and was a spring campaign, contrary to SWINGS and KEOPS (late summer campaigns). Noteworthy, the values for the WW over the plateau are similar to the outside-plateau WW (Table 2) and are not impacted by this anomaly restricted to ML only.

However, we note that the biogenic Si isotopic signatures of the plateau stations ($\delta^{30}Si_{BSi}$) in the ML are not necessarily lighter than the outside-plateau stations (1.58‰ for Station 44 and 2.00‰ at Station 68, Fig. 3b) and are close to $\delta^{30}Si_{DSi}$ plateau signatures. In light of the proximity of the bottom

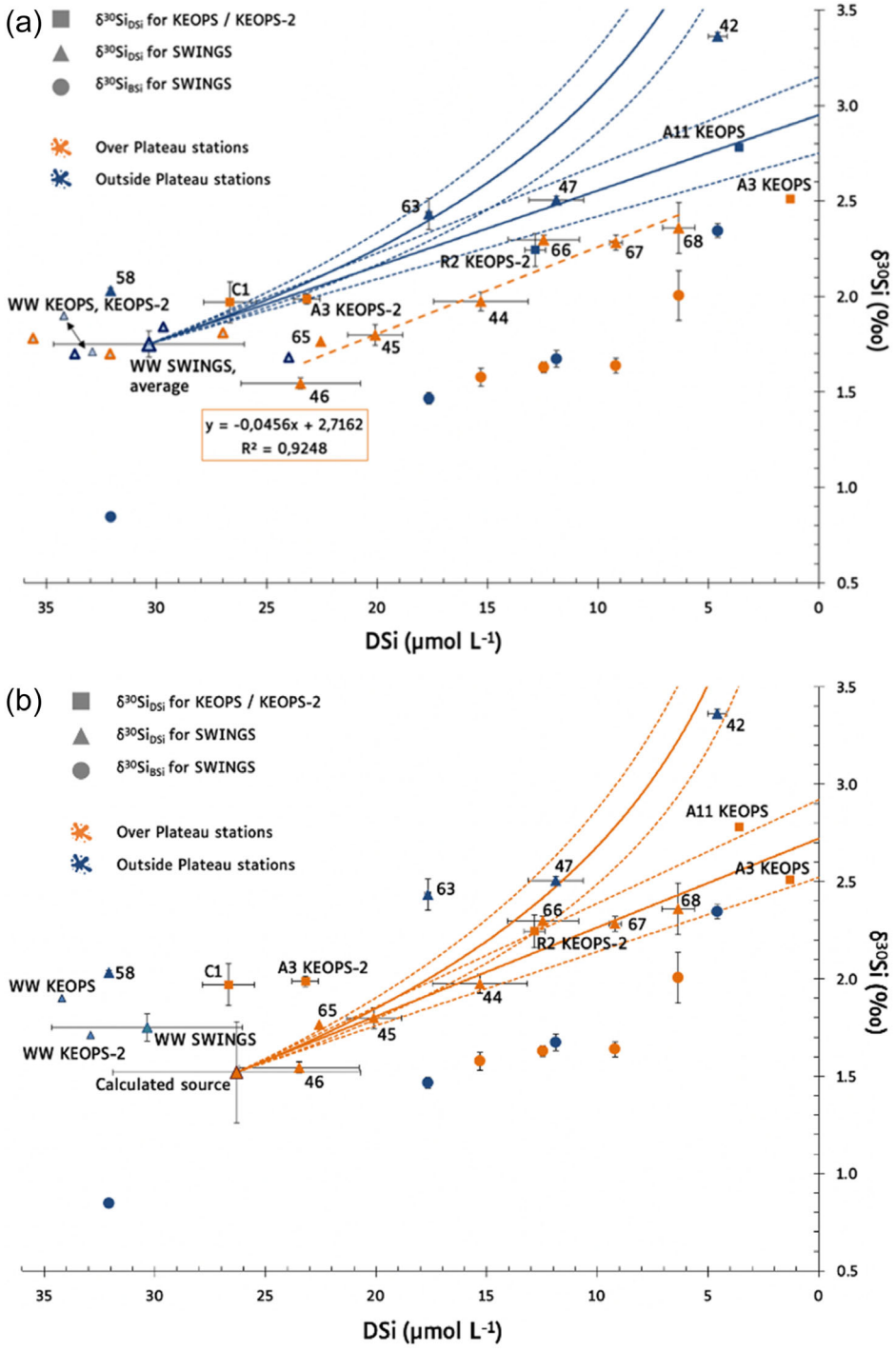

Fig. 3. $\delta^{30}Si$ (‰) vs. dissolved Si concentrations (μmol L^{-1}) in the mixed layer for on-plateau stations (orange triangles for $\delta^{30}Si_{DSi}$ and orange circles for $\delta^{30}Si_{BSi}$), outside-plateau stations (blue triangles for $\delta^{30}Si_{DSi}$ and blue circles for $\delta^{30}Si_{BSi}$), KEOPS (Fripiat et al. 2011b) and KEOPS-2 (Closset et al. 2016) stations (squares) as well as for respective WW (light blue triangles). (**a**) Blue curves represent the steady state and Rayleigh models for a single WW SWINGS source (30.3 $\pm$ 4.3 μmol L^{-1}; 1.75‰ $\pm$ 0.07‰) and a fractionation factor of -1.2‰ (solid curves) $\pm$ 0.2‰ (dashed curves). The dashed orange curve represents the linear correlation for the SWINGS on plateau stations. (**b**) Orange curve represents the steady state and Rayleigh models for a single on-plateau source as calculated in Supporting Information Text S6, for a fractionation factor of -1.2‰ (solid curves) $\pm$ 0.2‰ (dashed curves).

and the intense mixing over the entire water column, the dissolved Si reservoir could be non-synchronous with the biogenic Si reservoir in the ML. Indeed, storms were frequently observed during the SWINGS campaign, particularly around HMI shoal. Therefore, biogenic Si isotopic signatures will not be discussed further. In the discussion, we focus on the possible origins of this dissolved Si isotopically light source.

Calculation of contributions from lithogenic silicon and winter water

This calculation is developed in Supporting Information Text S6. We can calculate the relative contributions of WW and lithogenic silicon (LSi) to this source with a lighter $\delta^{30}Si$ signature:

$$x\delta^{30}Si_{LSi} + (1-x)\delta^{30}Si_{WW} = \delta^{30}Si_{DSi,\text{calculated plateau source}} \quad (1)$$

with, x = proportion coming from dissolution of LSi; $\delta^{30}Si_{L\text{-}Si}$ = $\delta^{30}Si$ signature of basalt = −0.4‰ ± 0.1‰, (Douthitt 1982; Georg et al. 2007); $\delta^{30}Si_{WW}$ = 1.75‰ ± 0.07‰ (Fig. 3, Table 2); $\delta^{30}Si_{DSi,\text{calculated plateau source}}$ = 1.52‰ ± 0.20‰ (Fig. 3b; Supporting Information Text S6).

The calculated contribution to ML dissolved Si from the dissolution of lithogenic Si is 11% ± 7% (error estimated from a Monte Carlo simulation with normal distribution, n = 1000). Indeed, the high uncertainty is due to the propagation of the isotopic variability of the plateau source, taken as a single average source for all the plateau stations.

Calculation of dissolution flux of lithogenic silicon around Heard and McDonald

Our study using Si isotopes can discriminate the contribution coming solely from the dissolution of lithogenic Si, enabling us to calculate the flux. We consider the source area of the isotopic anomaly on the Kerguelen Plateau to be 748 km^2, corresponding to the area with a bathymetry of maximum 100 m where the isotopic anomaly is visible (i.e., Stations 44, 45, 46, and 65; Supporting Information Fig. S6). The average depth in this selected area is 53 m, and the average residence time from the station near Heard Island to Station 44 is estimated at 15 d (Supporting Information Fig. S6). We can thus calculate the Si flux that would be delivered by this coastal lithogenic Si source to the ML. The concentration of Si coming from the dissolution of lithogenic Si being estimated at 2.9 ± 1.8 μmol L^{-1} (*see* previous section Calculation of contributions from lithogenic silicon and WW), we calculated the Si flux around HMI as follows:

$$\text{Flux}_{\text{dissolution of LSi Kerguelen}} = \frac{[DSi_{LSi}] \times \text{Volume}_{\text{plateau}(0-100)}}{\text{Residence time}_{\text{plateau}}} \quad (2)$$

with, $[DSi_{\text{from LSi}}]$ = 2.9 ± 1.8 × 10^{-3} mol m^{-3}; $\text{Volume}_{\text{anomaly plateau (0–100)}}$ = 53 × 748 × 10^6 = 396 × 10^8 m^3; Residence Time = 15 ± 2 d = 0.041 ± 0.005 yr.

The dissolution lithogenic Si flux around HMI equals 2.8 ± 1.8 × 10^9 mol yr^{-1}, corresponding to a specific flux of 3.7 ± 2.3 × 10^6 mol km^{-2} yr^{-1}.

Discussion

Two major Si sources over the Kerguelen plateau: Winter water and lithogenic silicon

To understand the contributions to the ML around the HMI, it is important to consider the contributions from the WW (*see* section Winter water) and from the dissolution of particulate Si. Isotopic biogenic Si signature in the ML ($\delta^{30}Si_{BSi,ML\ plateau}$ = 1.71‰ ± 0.20 ‰) is not significantly different from the dissolved Si isotopic in the WW ($\delta^{30}Si_{DSi\ WW}$ = 1.75‰ ± 0.07‰, Table 2). This is expected since dissolved Si in the WW results from the biogenic Si dissolution process: indeed, any nutrient contents below the surface are the result of cumulated remineralization processes during the water mass journey (neglecting the preformed contribution). We therefore assume that the isotopic anomaly observed is due solely to the dissolution of a non-BSi particulate Si pool that is likely to be lithogenic Si from HMI. Indeed, a significant amount of lithogenic Si (> 150 mmol m^{-2} integrated over the 200 m) is observed around Heard (Stations 44, 45, and 46) and McDonald Island (Station 65), while the integrated lithogenic Si concentration is moderate in the center of the Kerguelen Plateau (< 50 mmol m^{-2} for Stations 66, 67, and 68; Deteix et al. 2024). It can be assumed that the lithogenic Si decreasing gradient between Heard Island and Station 68 is mostly due to settling, but also that a small lithogenic Si fraction can be dissolved and transported along the pathway of water parcels associated with the circulation over the plateau, as mentioned just above.

Around HMI, the lithogenic Si can be of different origins:

i. Volcanic ash since Heard and McDonald are two volcanically active islands that could generate plume of airborne volcanic ash which eventually dissolves. With an assumed isotopic composition similar to basalt (−0.38‰, Opfergelt et al. 2010), ash dissolution could bring isotopically light dissolved Si to the water column. Indeed, volcanic ashes were observed in our mixed layer samples (Deteix et al. 2024).
ii. Primary minerals since feldspars and amphiboles have also been observed in our samples (Deteix et al. 2024), in accordance with the basaltic nature of the Kerguelen Plateau. The impact of minerals (probably including feldspars too) from terranes in Patagonia has been reported on the isotopic composition of $\delta^{30}Si$ (< 0.45 μm, Pryer et al. 2020), similar to this study.
iii. Glacial weathering can be a source of ocean-reactive detrital material from glacial flour as observed in Arctic fjord, with a probable impact on coastal $\delta^{30}Si$, where a slight isotopic anomaly has been identified too: such glacial weathering can supply very fine primary minerals along

with amorphous Si (Hatton et al. 2023). Note that Heard and Kerguelen Islands have a glacier but Mc Donald does not.

iv. Benthic LSi dissolution could originate from submarine basalt weathering, including from hydrothermalism (Tréguer et al. 2021) and/or direct interaction with coast such as sandy beaches (Aparicio et al. 2025) or even LSi in sediments as recently suggested in Antarctic shelf environments (Cassarino et al. 2020) or in open Southern Ocean (Closset et al. 2022) from measurements of δ^{30}Si in pore water.

During the KEOPS survey, the lithogenic silicon (LSi) fraction was estimated to be 32% ± 8% of the total particulate Si at Heard Island (Mosseri et al. 2008). Similarly, during the SWINGS cruise near Heard Island (Stations 45 and 46) and McDonald Island (Station 65), the fraction of lithogenic Si was 42% ± 11% and 30% ± 5%, respectively (Deteix et al. 2024). The Kerguelen Plateau, being a large basaltic igneous province (Freise et al. 2009), allows us to hypothesize that lithogenic Si dissolution is mostly of basaltic origin (Fripiat et al. 2011b), and indeed all LSi sources above could supply LSi with a basaltic-derived δ^{30}Si signature.

Contributions from lithogenic silicon and winter water

Since we have discussed that the Si source to the ML over the plateau has likely two origins, WW and LSi, we calculated the isotopic composition of this source (11% ± 7%; *see* section Calculation of contributions from lithogenic silicon and WW) to fit the ML $\delta^{30}Si_{DSi}$ (Fig. 3b). Therefore, the resulting lithogenic Si contribution is an average value that includes the variability among the plateau stations. This proportion combined with the calculated source concentration (26.3 ± 5.6 μmol L^{-1}), corresponds to a dissolved Si input of 23.4 ± 1.8 μmol L^{-1} from the WW and 2.9 ± 1.8 μmol L^{-1} from the dissolution of lithogenic Si. This result is in agreement with that obtained during KEOPS near Heard Island established at 2.6 ± 1.3 μmol L^{-1} or 10% ± 5% coming from LSi too. This initial estimate was based on few measurements in the ML of only one station (Fripiat et al. 2011b) while ours integrates the data from all SWINGS plateau stations (Eq. 1). Similarly, a contribution of 10% from basalt alteration has been tested with modeling on the Kerguelen Plateau and appears to be consistent (Coffineau et al. 2014). However, no distinction can be made between dissolution either directly from the lithogenic Si in sediment, or from the oceanic crust weathering or from dissolution within the water column.

Since the WW over the Plateau shows no isotopic anomaly, this indicates that the lithogenic Si dissolution is significant only in the upper 150 m around HMI. This could then fertilize the inner part of the shelf and give rise to the bloom observed in particular at Station 66. To explain the position of the bloom which is not taking place in the coastal areas but is located further north of Heard (Supporting Information Fig. S1), Van Beek et al. (2008) suggested for the KEOPS cruise that bathymetry plays a crucial role, constraining primary production and limiting it immediately around HMI due to intense mixing and turbulence. Dissolved elements from particles can then be transported to the surface via the geostrophic current on the Kerguelen Plateau (Fig. 1; Park et al. 2008). In the following, we now estimate the lithogenic Si dissolution fluxes.

Dissolution flux of lithogenic silicon around Heard and McDonald

The use of silicon isotopes makes it possible to isolate the contribution from the dissolution of lithogenic silicon. The resulting flux from the environments around HMI is calculated in section Calculation of dissolution flux of lithogenic silicon around Heard and McDonald (2.8 ± 1.8 × 10^9 mol yr^{-1}, corresponding to a specific flux of 3.7 ± 2.3 × 10^6 mol km^{-2} yr^{-1}). Recent studies have shown that detrital (i.e., subglacial amorphous Si) material is supplying dissolved Si to diatoms in glaciated margins (e.g., off Greenland; Ng et al. 2024). Similarly, several experiments have reported significant dissolution of river sediments (Oelkers et al. 2011; Jones et al. 2012). In our case, the studies by Cheize et al. (2019), Pearce et al. (2013) and Morin et al. (2015) are particularly interesting as they consider basaltic material in seawater. The silicon solubility of such basaltic particles can reach 0.17% over a period of around a few months for basalts in Kerguelen sediments (Pearce et al. 2013) or even 0.33% ± 0.04% for Heard Island basaltic sediments resuspended in seawater (Cheize et al. 2019). This dissolution can have a significant impact on primary production (Jeandel et al. 2011). Similarly, Geisen et al. (2022) report a Si solubility of 1.25% ± 0.51% and 0.11% ± 0.05% of desert dust and volcanic ash aerosols (dry deposition), respectively, after 48 h in natural Kerguelen area surface seawater, both aerosols containing feldspars; such Si supply induced a significant increase in diatoms and primary production in microcosm incubations from Kerguelen Plateau.

Supporting Information Table S2 compiles some of the global and regional Si fluxes of lithogenic origin to the ocean and shows great variability. In the global ocean, the dissolution flux of lithogenic Si from the weathering of basaltic oceanic crust has been estimated at 1.9 ± 0.7 × 10^{12} mol yr^{-1} (Tréguer et al. 2021). This flux includes the dissolution of terrestrial lithogenic material brought by erosion from rivers on shelves that are not differentiated from the alteration of oceanic basalt crust. Dissolved Si fluxes from oceanic basalt are indeed among the most poorly constrained in the marine Si cycle, and Frings (2017) estimates a global specific flux 10 times higher than Tréguer et al. (2021). These global fluxes are not focused on shallow areas, and they use a very large surface (including e.g., carbonate ooze sediments), which decreases dramatically the specific flux. Focusing on coastal areas, a recent study reports a global Si supply from the

dissolution of sandy beaches to the ocean similar to that of rivers (Aparicio et al. 2025; Supporting Information Table S2), a process that was already highlighted by measurements of the Si isotopic composition of the surrounding waters (Ehlert et al. 2016; Supporting Information Table S2) but not quantified globally.

Comparison with regional and global specific lithogenic silicon dissolution fluxes

Our Si specific flux estimate based on Si isotopic anomaly is much higher than the specific fluxes estimated globally on opal-poor sediment by Tréguer et al. (1995; 2021; by a factor of ×270 and ×140, respectively) and 20 times higher than the global estimate of Frings (2017). This reflects first the high uncertainty of the global Si fluxes to the ocean but most probably also the particularity of the Heard and McDonald region. Indeed, our specific flux is comparable to the Si dissolution flux from simulated volcanic ash dry deposition (single event of 25 mg ash L^{-1}; Geisen et al. 2022) while being two orders of magnitude higher than the one measured from simulated resuspended Heard sediment (5 mg sediment L^{-1}; Cheize et al. 2019). This suggests that fresh lithogenic material, including volcanic ashes from Heard and McDonald to the surrounding coastal zones, is more likely to be the cause of the Si isotopic anomaly than only the strong connection between shallow sediment and the ML with the intense mixing of the water column. Indeed, the nepheloid may remobilize lithogenic material already weathered that releases relatively less Si, as reported by Cheize et al. (2019).

Recently, diffusive fluxes of dissolved Si to the bottom waters from interstitial waters have been estimated at 3.2 $\times 10^4$ to 5.5 $\times 10^4$ mol km^{-2} yr^{-1} from the dissolution of lithogenic Si in the HNLC Antarctic zone (Closset et al. 2022). These fluxes are much lower than ours, which is expected since they are based on open ocean deep Southern Ocean sediments. The amount of lithogenic Si resuspended on the plateau, particularly in Heard and McDonald areas, is obviously greater than in the open ocean HNLC zone, as confirmed by the presence of primary minerals and volcanic ashes in our shallow samples (Deteix et al. 2024). Mixing is particularly intense at Heard and McDonald Stations, likely favoring greater dissolution (Jeandel 2016; Aparicio et al. 2025). At this stage, it is difficult to ascertain whether subglacial and/or volcanic supply dominates our additional Si source, but both have been shown from previous studies to possibly supply significant dissolved Si to diatoms (Ng et al. 2024; Geisen et al. 2022).

Indeed, subglacial specific Si fluxes from the northern high latitudes are also very variable but could reach a magnitude approaching ours (*see* the higher limit of Ng et al. 2020 estimate compiled in Supporting Information Table S2). Since McDonald Island is ice-free, the common feature with HMI is the presence of active volcanoes which would favor the hypothesis on the significant role of volcanic ashes. Heard and McDonald Islands volcanic aerosols have previously been identified as Fe suppliers to the surrounding waters (Perron et al. 2021). Noteworthy, van der Merwe et al. (2019) report that subglacial erosion is a significant source of Fe around Heard, while active hydrothermalism could be the main process for Fe supply around McDonald. Our very high specific Si flux estimate for HMI stations of SWINGS could therefore result from a combination of these particular processes in the area (volcanism, subglacial erosion, maybe also hydrothermalism). Further studies would be needed, focusing on quantifying HMI volcanic aerosol fluxes and fate, Si solubility of fresh continental eroded material (including subglacial particles from Heard), as well as implementing a survey on submarine hydrothermalism and/or basalt weathering. Our study confirms the recent interest in studying the land-to-ocean continuum in polar environments to better constrain the Si fluxes and their biogeochemical impacts in the ocean (Jankowski et al. 2023), including the use of Si isotopes (e.g., Hirst et al. 2020; Brzezinski et al. 2021; Hendry et al. 2025).

Author Contributions

Damien Cardinal: Project supervision, administration, and funding acquisition. Edwin Cotard and Damien Cardinal: Conceptualization of the project and investigation. Edwin Cotard, Valentin Deteix, and Arnaud Dapoigny: Data acquisition, validation, and statistical analyses. Edwin Cotard, Valentin Deteix, and Frédéric Vivier: Data presentation and figures. Edwin Cotard and Damien Cardinal: Initial draft preparation. Edwin Cotard, Valentin Deteix, Frédéric Vivier, Sandrine Caquineau, and Damien Cardinal: Writing, review, and editing.

Acknowledgments

We would like to thank Captain A. Eyssautier, LDA and GENAVIR staff and the crew of the R/V *Marion Dufresne* for their help during the SWINGS cruise. We warmly thank the chief scientists Catherine Jeandel and Hélène Planquette, Emmanuel de Saint-Léger and Fabien Pérault (CNRS DT INSU). We are grateful to Marine Piéjus for on-board sampling and filtering; Mustapha Benrahmoune (LOCEAN) for managing the clean laboratory; Pierre Burckel and the PARI analytical platform (IPGP) for ICP-MS; Stéphanie Jacquet for providing on-board filtration units; Irina Djouraev and the Alysés analytical platform (IRD-SU) for ICP-MS; the PANOPLY analytical platform (CNRS-CEA-Université Paris Sud-UVSQ) for MC-ICP-MS analysis; Catherine Schmechtig and the LEFE-CYBER Database for data accessibility of previous oceanographic missions. Maps were drawn with the M_Map Matlab toolbox (Pawlowicz 2020). This study has been conducted using E.U. Copernicus Marine Service Information. Finally, we thank K. Hendry and an anonymous reviewer for their constructive and positive comments that helped to improve this manuscript. The SWINGS

project was supported by the Flotte Océanographique Française (10.17600/18001925), Agence Nationale de la Recherche (ANR 19-CE01-0012), CNRS/INSU (Centre National de la Recherche Scientifique/Institut National des Sciences de l'Univers) through its LEFE actions, Université de Bretagne Occidentale, and IsBlue project, Interdisciplinary graduate school for the blue planet (ANR 17-EURE-0015).

Conflicts of Interest

None declared.

Data Availability Statement

Data available in the article, Supporting Information, and accessible via two DOIs: For the stable isotopic composition of biogenic and dissolved silicon (δ^{30}Si): https://doi.org/10.17882/105453. For lithogenic and biogenic silicon concentrations: https://doi.org/10.17882/97947.

References

Aparicio, M., A. Le Bihan, C. Jeandel, S. Fabre, R. Almar, and I. M. Mingo. 2025. "Contribution of Sandy Beaches to the Global Marine Silicon Cycle." *Nature Geoscience* 18: 154–159. https://doi.org/10.1038/s41561-024-01628-6.

Armand, L. K., V. Cornet-Barthaux, J. Mosseri, and B. Quéguiner. 2008. "Late Summer Diatom Biomass and Community Structure On and Around the Naturally Iron-Fertilised Kerguelen Plateau in the Southern Ocean." *Deep Sea Research Part II: Topical Studies in Oceanography* 55: 653–676. https://doi.org/10.1016/j.dsr2.2007.12.031.

Armand, L. K., X. Crosta, O. Romero, and J.-J. Pichon. 2005. "The Biogeography of Major Diatom Taxa in Southern Ocean Sediments." *Palaeogeography Palaeoclimatology Palaeoecology* 223: 93–126. https://doi.org/10.1016/j.palaeo.2005.02.015.

Blain, S., J. Capparos, A. Guéneuguès, I. Obernosterer, and L. Oriol. 2015. "Distributions and Stoichiometry of Dissolved Nitrogen and Phosphorus in the Iron-Fertilized Region Near Kerguelen (Southern Ocean)." *Biogeosciences* 12: 623–635. https://doi.org/10.5194/bg-12-623-2015.

Blain, S., B. Quéguiner, L. Armand, et al. 2007. "Effect of Natural Iron Fertilization on Carbon Sequestration in the Southern Ocean." *Nature* 446: 1070–1074. https://doi.org/10.1038/nature05700.

Bouttes, N., D. Paillard, D. M. Roche, et al. 2012. "Impact of Oceanic Processes on the Carbon Cycle During the Last Termination." *Climate of the Past* 8: 149–170. https://doi.org/10.5194/cp-8-149-2012.

Brzezinski, M. A., I. Closset, J. L. Jones, G. F. De Souza, and C. Maden. 2021. "New Constraints on the Physical and Biological Controls on the Silicon Isotopic Composition of the Arctic Ocean." *Frontiers in Marine Science* 8: 699762. https://doi.org/10.3389/fmars.2021.699762.

Brzezinski, M. A., D. M. Nelson, V. M. Franck, and D. E. Sigmon. 2001. "Silicon Dynamics Within an Intense Open-Ocean Diatom Bloom in the Pacific Sector of the Southern Ocean." *Deep Sea Research Part II: Topical Studies in Oceanography* 48: 3997–4018. https://doi.org/10.1016/S0967-0645(01)00078-9.

Buesseler, K. O., L. Ball, J. Andrews, et al. 2001. "Upper Ocean Export of Particulate Organic Carbon and Biogenic Silica in the Southern Ocean along 170°W." *Deep Sea Research Part II: Topical Studies in Oceanography* 48: 4275–4297. https://doi.org/10.1016/S0967-0645(01)00089-3.

Cardinal, D., L. Y. Alleman, F. Dehairs, N. Savoye, T. W. Trull, and L. André. 2005. "Relevance of Silicon Isotopes to Si-Nutrient Utilization and Si-Source Assessment in Antarctic Waters: Silicon Isotopes in Antarctic Waters." *Global Biogeochemical Cycles* 19: GB2007. https://doi.org/10.1029/2004GB002364.

Cardinal, D., N. Savoye, T. W. Trull, et al. 2007. "Silicon Isotopes in Spring Southern Ocean Diatoms: Large Zonal Changes Despite Homogeneity Among Size Fractions." *Marine Chemistry* 106: 46–62. https://doi.org/10.1016/j.marchem.2006.04.006.

Cassarino, L., K. R. Hendry, S. F. Henley, et al. 2020. "Sedimentary Nutrient Supply in Productive Hot Spots Off the West Antarctic Peninsula Revealed by Silicon Isotopes." *Global Biogeochemical Cycles* 34: e2019GB006486. https://doi.org/10.1029/2019GB006486.

Cavagna, A.-J., F. Fripiat, F. Dehairs, et al. 2011. "Silicon Uptake and Supply During a Southern Ocean Iron Fertilization Experiment (EIFEX) Tracked by Si Isotopes." *Limnology and Oceanography* 56: 147–160. https://doi.org/10.4319/lo.2011.56.1.0147.

Cheize, M., H. F. Planquette, J. N. Fitzsimmons, et al. 2019. "Contribution of Resuspended Sedimentary Particles to Dissolved Iron and Manganese in the Ocean: An Experimental Study." *Chemical Geology* 511: 389–415. https://doi.org/10.1016/j.chemgeo.2018.10.003.

Closset, I., M. A. Brzezinski, D. Cardinal, A. Dapoigny, J. L. Jones, and R. S. Robinson. 2022. "A Silicon Isotopic Perspective on the Contribution of Diagenesis to the Sedimentary Silicon Budget in the Southern Ocean." *Geochimica et Cosmochimica Acta* 327: 298–313. https://doi.org/10.1016/j.gca.2022.04.010.

Closset, I., D. Cardinal, S. G. Bray, et al. 2015. "Seasonal Variations, Origin, and Fate of Settling Diatoms in the Southern Ocean Tracked by Silicon Isotope Records in Deep Sediment Traps." *Global Biogeochemical Cycles* 29: 1495–1510. https://doi.org/10.1002/2015GB005180.

Closset, I., D. Cardinal, M. Rembauville, F. Thil, and S. Blain. 2016. "Unveiling the Si Cycle Using Isotopes in an Iron-Fertilized Zone of the Southern Ocean: From Mixed-Layer Supply to Export." *Biogeosciences* 13: 6049–6066. https://doi.org/10.5194/bg-13-6049-2016.

Closset, I., M. Lasbleiz, K. Leblanc, et al. 2014. "Seasonal Evolution of Net and Regenerated Silica Production Around a

Natural Fe-Fertilized Area in the Southern Ocean Estimated With Si Isotopic Approaches." *Biogeosciences* 11: 5827–5846. https://doi.org/10.5194/bg-11-5827-2014.

Coffineau, N., C. L. De La Rocha, and P. Pondaven. 2014. "Exploring Interacting Influences on the Silicon Isotopic Composition of the Surface Ocean: A Case Study From the Kerguelen Plateau." *Biogeosciences* 11: 1371–1391. https://doi.org/10.5194/bg-11-1371-2014.

De Boyer Montégut, C., G. Madec, A. S. Fischer, A. Lazar, and D. Iudicone. 2004. "Mixed Layer Depth Over the Global Ocean: An Examination of Profile Data and a Profile-Based Climatology." *Journal of Geophysical Research: Oceans* 109, no. C12: 2004JC002378. https://doi.org/10.1029/2004JC002378.

De La Rocha, C. L., P. Bescont, A. Croguennoc, and E. Ponzevera. 2011. "The Silicon Isotopic Composition of Surface Waters in the Atlantic and Indian Sectors of the Southern Ocean." *Geochimica et Cosmochimica Acta* 75: 5283–5295. https://doi.org/10.1016/j.gca.2011.06.028.

de la Rocha, C. L., M. A. Brzezinski, and M. J. DeNiro. 1997. "Fractionation of Silicon Isotopes by Marine Diatoms During Biogenic Silica Formation." *Geochimica et Cosmochimica Acta* 61: 5051–5056. https://doi.org/10.1016/S0016-7037(97)00300-1.

Deteix, V., E. Cotard, S. Caquineau, et al. 2024. "Biogenic and Lithogenic Silicon Along the GEOTRACES South West Indian Ocean Section (SWINGS-GS02) and the Islands Mass Effect on Regional Si Biogeochemical Cycle." *Marine Chemistry* 263: 104412. https://doi.org/10.1016/j.marchem.2024.104412.

Douthitt, C. B. 1982. "The Geochemistry of the Stable Isotopes of Silicon." *Geochimica et Cosmochimica Acta* 46: 1449–1458. https://doi.org/10.1016/0016-7037(82)90278-2.

Dugdale, R. C., F. P. Wilkerson, and H. J. Minas. 1995. "The Role of a Silicate Pump in Driving New Production." *Deep Sea Research, Part I: Oceanographic Research Papers* 42: 697–719. https://doi.org/10.1016/0967-0637(95)00015-X.

Ehlert, C., A. Reckhardt, J. Greskowiak, et al. 2016. "Transformation of Silicon in a Sandy Beach Ecosystem: Insights From Stable Silicon Isotopes From Fresh and Saline Groundwaters." *Chemical Geology* 440: 207–218. https://doi.org/10.1016/j.chemgeo.2016.07.015.

Freise, M., F. Holtz, M. Nowak, J. S. Scoates, and H. Strauss. 2009. "Differentiation and Crystallization Conditions of Basalts From the Kerguelen Large Igneous Province: An Experimental Study." *Contributions to Mineralogy and Petrology* 158: 505–527. https://doi.org/10.1007/s00410-009-0394-5.

Frings, P. 2017. "Revisiting the Dissolution of Biogenic Si in Marine Sediments: A Key Term in the Ocean Si Budget." *Acta Geochimica* 36: 429–432. https://doi.org/10.1007/s11631-017-0183-1.

Fripiat, F., A.-J. Cavagna, F. Dehairs, S. Speich, L. André, and D. Cardinal. 2011*a*. "Silicon Pool Dynamics and Biogenic Silica Export in the Southern Ocean Inferred From Si-Isotopes." *Ocean Science* 7: 533–547. https://doi.org/10.5194/os-7-533-2011.

Fripiat, F., A.-J. Cavagna, N. Savoye, F. Dehairs, L. André, and D. Cardinal. 2011*b*. "Isotopic Constraints on the Si-Biogeochemical Cycle of the Antarctic Zone in the Kerguelen Area (KEOPS)." *Marine Chemistry* 123: 11–22. https://doi.org/10.1016/j.marchem.2010.08.005.

Geisen, C., C. Ridame, E. Journet, et al. 2022. "Phytoplanktonic Response to Simulated Volcanic and Desert Dust Deposition Events in the South Indian and Southern Oceans." *Limnology and Oceanography* 67: 1537–1553. https://doi.org/10.1002/lno.12100.

Georg, R. B., A. N. Halliday, E. A. Schauble, and B. C. Reynolds. 2007. "Silicon in the Earth's Core." *Nature* 447: 1102–1106. https://doi.org/10.1038/nature05927.

Grasse, P., M. A. Brzezinski, D. Cardinal, et al. 2017. "GEOTRACES Inter-Calibration of the Stable Silicon Isotope Composition of Dissolved Silicic Acid in Seawater." *Journal of Analytical Atomic Spectrometry* 32: 562–578. https://doi.org/10.1039/C6JA00302H.

Hatton, J. E., H. C. Ng, L. Meire, et al. 2023. "Silicon Isotopes Highlight the Role of Glaciated Fjords in Modifying Coastal Waters." *Journal of Geophysical Research—Biogeosciences* 128: e2022JG007242. https://doi.org/10.1029/2022JG007242.

Heimburger, A., R. Losno, S. Triquet, and E. B. Nguyen. 2013. "Atmospheric Deposition Fluxes of 26 Elements Over the Southern Indian Ocean: Time Series on Kerguelen and Crozet Islands." *Global Biogeochemical Cycles* 27: 440–449. https://doi.org/10.1002/gbc.20043.

Hendry, K. R., F. de Sales Freitas, S. Arndt, et al. 2025. "Insights Into Silicon Cycling From Ice Sheet to Coastal Ocean From Isotope Geochemistry." *Communications Earth & Environment* 6: 305. https://doi.org/10.1038/s43247-025-02264-7.

Hirst, C., S. Opfergelt, F. Gaspard, et al. 2020. "Silicon Isotopes Reveal a Non-Glacial Source of Silicon to Crescent Stream, McMurdo Dry Valleys, Antarctica." *Frontiers in Earth Science* 8: 229. https://doi.org/10.3389/feart.2020.00229.

Jankowski, K. J., K. Johnson, L. Sethna, et al. 2023. "Long-Term Changes in Concentration and Yield of Riverine Dissolved Silicon From the Poles to the Tropics." *Global Biogeochemical Cycles* 37: e2022GB007678. https://doi.org/10.1029/2022GB007678.

Jeandel, C. 2016. "Overview of the Mechanisms That Could Explain the 'Boundary Exchange' at the Land–Ocean Contact." *Philosophical Transactions of the Royal Society A: Mathematical, Physical and Engineering Sciences* 374: 20150287. https://doi.org/10.1098/rsta.2015.0287.

Jeandel, C., B. Peucker-Ehrenbrink, M. T. Jones, et al. 2011. "Ocean Margins: The Missing Term in Oceanic Element Budgets?" *Eos, Transactions American Geophysical Union* 92: 217–218. https://doi.org/10.1029/2011EO260001.

Jones, M. T., C. R. Pearce, and E. H. Oelkers. 2012. "An Experimental Study of the Interaction of Basaltic Riverine

Particulate Material and Seawater." *Geochimica et Cosmochimica Acta* 77: 108–120. https://doi.org/10.1016/j.gca.2011.10.044.

Karl, D. M., and G. Tien. 1992. "MAGIC: A Sensitive and Precise Method for Measuring Dissolved Phosphorus in Aquatic Environments." *Limnology and Oceanography* 37: 105–116. https://doi.org/10.4319/lo.1992.37.1.0105.

Khatiwala, S., F. Primeau, and T. Hall. 2009. "Reconstruction of the History of Anthropogenic CO_2 Concentrations in the Ocean." *Nature* 462: 346–349. https://doi.org/10.1038/nature08526.

Kopczyńska, E. E., N. Savoye, F. Dehairs, D. Cardinal, and M. Elskens. 2007. "Spring Phytoplankton Assemblages in the Southern Ocean Between Australia and Antarctica." *Polar Biology* 31: 77–88. https://doi.org/10.1007/s00300-007-0335-6.

Moore, J. K., S. C. Doney, D. M. Glover, and I. Y. Fung. 2001. "Iron Cycling and Nutrient-Limitation Patterns in Surface Waters of the World Ocean." *Deep Sea Research, Part II: Topical Studies in Oceanography* 49: 463–507. https://doi.org/10.1016/S0967-0645(01)00109-6.

Moore, J. K., S. C. Doney, and K. Lindsay. 2004. "Upper Ocean Ecosystem Dynamics and Iron Cycling in a Global Three-Dimensional Model." *Global Biogeochemical Cycles* 18: 2004GB002220. https://doi.org/10.1029/2004GB002220.

Morin, G. P., N. Vigier, and A. Verney-Carron. 2015. "Enhanced Dissolution of Basaltic Glass in Brackish Waters: Impact on Biogeochemical Cycles." *Earth and Planetary Science Letters* 417: 1–8. https://doi.org/10.1016/j.epsl.2015.02.005.

Mosseri, J., B. Quéguiner, L. Armand, and V. Cornet-Barthaux. 2008. "Impact of Iron on Silicon Utilization by Diatoms in the Southern Ocean: A Case Study of Si/N Cycle Decoupling in a Naturally Iron-Enriched Area." *Deep Sea Research Part II: Topical Studies in Oceanography* 55: 801–819. https://doi.org/10.1016/j.dsr2.2007.12.003.

Ng, H. C., L. Cassarino, R. A. Pickering, E. M. S. Woodward, S. J. Hammond, and K. R. Hendry. 2020. "Sediment Efflux of Silicon on the Greenland Margin and Implications for the Marine Silicon Cycle." *Earth and Planetary Science Letters* 529: 115877. https://doi.org/10.1016/j.epsl.2019.115877.

Ng, H. C., K. R. Hendry, R. Ward, et al. 2024. "Detrital Input Sustains Diatom Production Off a Glaciated Arctic Coast." *Geophysical Research Letters* 51: e2024GL108324. https://doi.org/10.1029/2024GL108324.

Oelkers, E. H., S. R. Gislason, E. S. Eiriksdottir, M. Jones, C. R. Pearce, and C. Jeandel. 2011. "The Role of Riverine Particulate Material on the Global Cycles of the Elements." *Applied Geochemistry* 26: S365–S369. https://doi.org/10.1016/j.apgeochem.2011.03.062.

Opfergelt, S., D. Cardinal, L. André, C. Delvigne, L. Bremond, and B. Delvaux. 2010. "Variations of δ^{30}Si and Ge/Si With Weathering and Biogenic Input in Tropical Basaltic Ash Soils Under Monoculture." *Geochimica et Cosmochimica Acta* 74: 225–240. https://doi.org/10.1016/j.gca.2009.09.025.

Park, Y.-H., E. Charriaud, and M. Fieux. 1998. "Thermohaline Structure of the Antarctic Surface Water/Winter Water in the Indian Sector of the Southern Ocean." *Journal of Marine Systems* 17: 5–23. https://doi.org/10.1016/S0924-7963(98)00026-8.

Park, Y.-H., I. Durand, E. Kestenare, et al. 2014. "Polar Front Around the Kerguelen Islands: An Up-To-Date Determination and Associated Circulation of Surface/Subsurface Waters." *Journal of Geophysical Research. Oceans* 119: 6575–6592. https://doi.org/10.1002/2014JC010061.

Park, Y.-H., T. Park, T.-W. Kim, et al. 2019. "Observations of the Antarctic Circumpolar Current Over the Udintsev Fracture Zone, the Narrowest Choke Point in the Southern Ocean." *Journal of Geophysical Research. Oceans* 124: 4511–4528. https://doi.org/10.1029/2019JC015024.

Park, Y.-H., F. Roquet, I. Durand, and J.-L. Fuda. 2008. "Large-Scale Circulation Over and Around the Northern Kerguelen Plateau." *Deep Sea Research Part II: Topical Studies in Oceanography* 55: 566–581. https://doi.org/10.1016/j.dsr2.2007.12.030.

Park, Y.-H., F. Vivier, F. Roquet, and E. Kestenare. 2009. "Direct Observations of the ACC Transport Across the Kerguelen Plateau." *Geophysical Research Letters* 36:L18603. https://doi.org/10.1029/2009GL039617.

Pawlowicz, R. 2020. M_Map: A Mapping Package for MATLAB. Computer Software.

Pearce, C. R., M. T. Jones, E. H. Oelkers, C. Pradoux, and C. Jeandel. 2013. "The Effect of Particulate Dissolution on the Neodymium (Nd) Isotope and Rare Earth Element (REE) Composition of Seawater." *Earth and Planetary Science Letters* 369–370: 138–147. https://doi.org/10.1016/j.epsl.2013.03.023.

Perron, M. M. G., B. C. Proemse, M. Strzelec, M. Gault-Ringold, and A. R. Bowie. 2021. "Atmospheric Inputs of Volcanic Iron Around Heard and McDonald Islands, Southern Ocean." *Environmental Science: Atmospheres* 1: 508–517. https://doi.org/10.1039/D1EA00054C.

Pryer, H. V., J. R. Hawkings, J. L. Wadham, et al. 2020. "The Influence of Glacial Cover on Riverine Silicon and Iron Exports in Chilean Patagonia." *Global Biogeochemical Cycles* 34: e2020GB006611. https://doi.org/10.1029/2020GB006611.

Quéguiner, B., and M. A. Brzezinski. 2002. "Biogenic Silica Production Rates and Particulate Organic Matter Distribution in the Atlantic Sector of the Southern Ocean During Austral Spring 1992." *Deep Sea Research Part II: Topical Studies in Oceanography* 49: 1765–1786. https://doi.org/10.1016/S0967-0645(02)00011-5.

Reynolds, B. C., J. Aggarwal, L. André, et al. 2007. "An Inter-Laboratory Comparison of Si Isotope Reference Materials." *Journal of Analytical Atomic Spectrometry* 22: 561–568. https://doi.org/10.1039/B616755A.

Reynolds, B., M. Frank, and A. Halliday. 2006. "Silicon Isotope Fractionation During Nutrient Utilization in the North

Pacific." *Earth and Planetary Science Letters* 244: 431–443. https://doi.org/10.1016/j.epsl.2006.02.002.

Sarmiento, J. L., N. Gruber, M. A. Brzezinski, and J. P. Dunne. 2004. "High-Latitude Controls of Thermocline Nutrients and Low Latitude Biological Productivity." *Nature* 427: 56–60. https://doi.org/10.1038/nature02127.

Sarmiento, J. L., J. Simeon, A. Gnanadesikan, N. Gruber, R. M. Key, and R. Schlitzer. 2007. "Deep Ocean Biogeochemistry of Silicic Acid and Nitrate." *Global Biogeochemical Cycles* 21: 2006GB002720. https://doi.org/10.1029/2006GB002720.

Schlitzer, R. 2024. Ocean data view.

Tagliabue, A., T. Mtshali, O. Aumont, et al. 2012. "A Global Compilation of Dissolved Iron Measurements: Focus on Distributions and Processes in the Southern Ocean." *Biogeosciences* 9: 2333–2349. https://doi.org/10.5194/bg-9-2333-2012.

Tréguer, P., C. Bowler, B. Moriceau, et al. 2018. "Influence of Diatom Diversity on the Ocean Biological Carbon Pump." *Nature Geoscience* 11: 27–37. https://doi.org/10.1038/s41561-017-0028-x.

Tréguer, P., D. M. Nelson, A. J. Van Bennekom, D. J. DeMaster, A. Leynaert, and B. Quéguiner. 1995. "The Silica Balance in the World Ocean: A Reestimate." *Science* 268: 375–379. https://doi.org/10.1126/science.268.5209.375.

Tréguer, P. J., and C. L. De La Rocha. 2013. "The World Ocean Silica Cycle." *Annual Review of Marine Science* 5: 477–501. https://doi.org/10.1146/annurev-marine-121211-172346.

Tréguer, P. J., J. N. Sutton, M. Brzezinski, et al. 2021. "Reviews and Syntheses: The Biogeochemical Cycle of Silicon in the Modern Ocean." *Biogeosciences* 18: 1269–1289. https://doi.org/10.5194/bg-18-1269-2021.

Trull, T., S. R. Rintoul, M. Hadfield, and E. R. Abraham. 2001. "Circulation and Seasonal Evolution of Polar Waters South of Australia: Implications for Iron Fertilization of the Southern Ocean." *Deep Sea Research Part II: Topical Studies in Oceanography* 48: 2439–2466. https://doi.org/10.1016/S0967-0645(01)00003-0.

Van Beek, P., M. Bourquin, J.-L. Reyss, M. Souhaut, M. A. Charette, and C. Jeandel. 2008. "Radium Isotopes to Investigate the Water Mass Pathways on the Kerguelen Plateau (Southern Ocean)." *Deep Sea Research Part II: Topical Studies in Oceanography* 55: 622–637. https://doi.org/10.1016/j.dsr2.2007.12.025.

van der Merwe, P., K. Wuttig, T. Holmes, et al. 2019. "High Lability Fe Particles Sourced From Glacial Erosion Can Meet Previously Unaccounted Biological Demand: Heard Island, Southern Ocean." *Frontiers in Marine Science* 6: 332. https://doi.org/10.3389/fmars.2019.00332.

Varela, D. E., C. J. Pride, and M. A. Brzezinski. 2004. "Biological Fractionation of Silicon Isotopes in Southern Ocean Surface Waters: Biological Fractionation of Silicon." *Global Biogeochemical Cycles* 18: GB1047. https://doi.org/10.1029/2003GB002140.

Wang, W.-L., W. Fu, F. A. C. Le Moigne, et al. 2023. "Biological Carbon Pump Estimate Based on Multidecadal Hydrographic Data." *Nature* 624: 579–585. https://doi.org/10.1038/s41586-023-06772-4.

Supporting Information

Additional Supporting Information may be found in the online version of this article.

Submitted 14 November 2024
Revised 21 May 2025
Accepted 12 October 2025